

Magnetic field measurements on the mini-ICAL detector using Hall probes

Honey,^{a,b,c,1} B. Satyanarayana,^b R. Shinde,^b V.M. Datar,^a D. Indumathi,^{a,c} Ram K V Thulasi,^b N. Dalal,^d S. Prabhakar,^d S. Ajith,^d Sourabh Pathak,^d Sandip Patel^d

^a*The Institute of Mathematical Sciences,
Taramani, Chennai 600113, India*

^b*Tata Institute of Fundamental Research,
Homi Bhabha Road, Mumbai 400005, India*

^c*Homi Bhabha National Institute,
Anushakti Nagar, Mumbai 400094, India*

^d*Bhabha Atomic Research Centre,
Mumbai 400085, India*

E-mail: honey@tifr.res.in

ABSTRACT: The magnetised 51 kton Iron Calorimeter (ICAL) detector proposed to be built at INO is designed with a focus on detecting 1-20 GeV muons. The magnetic field will enable the measurement of the momentum of the μ^- and μ^+ generated from the charge current interactions of ν_μ and $\bar{\nu}_\mu$ separately within iron in the detector, thus permitting the determination of the neutrino mass ordering/hierarchy, among other important goals of ICAL. Hence it is important to determine the magnetic field as accurately as possible. The mini-ICAL detector is an 85-ton prototype of ICAL, which is operational at Madurai in South India. We describe here the first measurement of the magnetic field in mini-ICAL using Hall sensor PCBs. A set-up developed to calibrate the Hall probe sensors using an electromagnet. The readout system has been designed using an Arduino Nano board for selection of channels of Hall probes mounted on the PCB and to convert the analog voltage to a digital output. The magnetic field has been measured in the small gaps (provided for the purpose) between iron plates in the top layer of mini-ICAL as well as in the air just outside the detector. A precision of better than 3% was obtained, with a sensitivity down to about 0.03 kGauss when measuring the small fringe fields outside the detector.

KEYWORDS: Magnetic field measurement, Arduino nano, electromagnet, Hall probe sensors

¹Corresponding author.

Contents

1	Introduction and Motivation	1
2	The mini-ICAL detector	2
2.1	The mini-ICAL geometry	3
2.2	Construction of the Hall probe	3
2.3	Experimental setup	4
3	Calibration of the Hall sensors	5
3.1	Measurement of the Offset Voltage	5
3.2	Calibration using gap dipole electro-magnet	6
4	Error Estimation	8
5	Measurement of the magnetic field in mini-ICAL	9
6	Fringe-field just outside mini-ICAL	10
7	Discussion and future plans	11
A	Calibration of Hall probe at 90⁰ dipole magnet at ECR ion source facility.	11

1 Introduction and Motivation

The proposed magnetized Iron Calorimeter (ICAL) detector to be located at the India-based Neutrino Observatory (INO) is designed to be a 51 kton iron detector optimized to detect μ^- and μ^+ generated from the charged current interactions within iron of ν_μ and $\bar{\nu}_\mu$ respectively in the energy range of few to 10s of GeV. The detector will comprise 3 modules made up of 151 layers of 56 mm thick iron plates with 150 layers of Resistive plate chambers (RPCs) as active detector element which are sandwiched between the iron plates. The magnetic field will be generated through current passing in copper coils which are wound around the iron plates in slots constructed for the purpose. Hence the field is expected to vary in both magnitude and direction over the area of the iron plates.

One of the most important capabilities of ICAL will be its ability to distinguish the sign of charged particles through the iron with a magnetic field of 1–1.5 T (10–15 kGauss) that will be generated using copper coils. Apart from helping to distinguish neutrino and anti-neutrino induced events, the magnetic field is also crucial to reconstruct the momenta (both magnitude and direction) of the muons produced in these interactions which is a critical input for the corresponding physics analyses [1],[2].

Simulations for the magnetic field using ICAL geometry have been performed using MAGNET software [3]. In order to validate these simulations and find the correlation between the estimated

magnetic field and the actual magnetic field, measurements are needed. Hence it is important to precisely measure and calibrate the magnetic field in ICAL.

To understand the challenges in the construction of such a huge detector, a small prototype detector called mini-ICAL has been set-up in Madurai, Tamil Nadu. The 85-ton detector, comprising 11 layers of iron with planar dimensions of $4 \times 4 \text{ m}^2$ in the x - y plane, has been magnetised to about 1 T using a current of 500 A. In each layer, the required geometry is achieved by the use of 7 iron plates of slightly varying dimensions, with small (2–3 mm) gaps between them. We report here for the first time, results of a study of the magnetic field generated in the mini-ICAL in a limited region of the detector, in particular, near these gaps where it is possible to insert appropriate probes.

There are various techniques which are available to measure magnetic fields, for example, SQUID, NMR, Magneto-resistance, Magneto-optical, Hall sensors, etc [4]. SQUIDs require very low temperature to operate while NMR, Magneto-resistance and Magneto-optical devices cannot be used due to their low range and scalar field measuring technique; hence these are not found suitable for our study. Hall sensors provide reasonably good accuracy and can measure fields over a wide range (100–10000 mT); therefore Hall sensors were chosen as the primary sensor to study the magnetic field in the mini-ICAL detector. In particular, the field measurement probe used in the current study was done at low cost (\sim US \$ 100). It was designed and constructed using inexpensive Hall sensors with sensitivity down to 10 mT and standard electronics. Since measurement and calibration of the magnetic field in the 151 layers of ICAL (when built) is likely to be a recurring activity, it was gratifying that the study showed consistency and could accurately measure the field in the small gaps/spaces between different iron plates in a layer. Even in regions such as in the air *just outside* the detector, where the magnetic field is expected to be small, of the order of 10s of Gauss, our measurements with different sensors were consistent to within 15–20 Gauss, which is close to the least count of the instrument.

We report here both on the magnetic field measurements in the air gap between iron plates in the top layer of mini-ICAL as well as just outside one of these gaps, in the air outside the detector. Some preliminary results were reported in Ref. [5]. The former is expected to be close to the value of the magnetic field in the adjoining iron layer. It will thus be possible to validate the estimates of the magnetic field obtained by the simulations. An actual simulation study of the mini-ICAL detector has not yet been done and is thus outside the scope of the present work.

We first describe the relevant geometry of the mini-ICAL detector before going on to describe the basic characteristics of Hall sensors, calibration of Hall sensors using an electromagnet and designing the Hall probe readout using Arduino Nano to extract the signals from Hall sensors. Finally, we report the first measurement of the magnetic field in the mini-ICAL detector.

2 The mini-ICAL detector

The mini-ICAL detector, see Fig. 1, is an 85-ton prototype magnetized detector located in Madurai, which detects cosmic muons. A magnetic field of upto 1.5 T can be produced in it with a current of 900 A, with upto 90% of its volume having a magnetic field of more than 1 T near saturation.

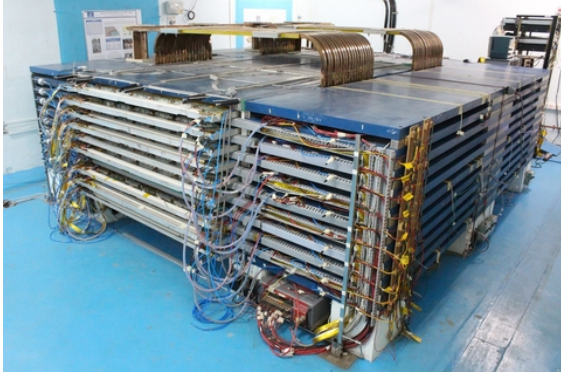


Figure 1. The mini-ICAL detector with 11 iron layers. The upper portion of copper coils and slots are clearly visible.

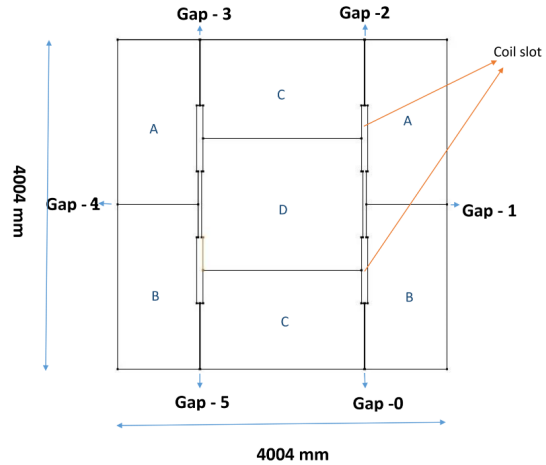


Figure 2. Schematic of top view of mini-ICAL showing the gaps 0, 2, 3, and 5. The B -field is dominantly in the x direction at these gaps.

2.1 The mini-ICAL geometry

The mini-ICAL consists of 11 layers of 56 mm thick iron plates with RPCs sandwiched in the 45 mm gap between them. Each iron layer is $4 \times 4 \text{ m}^2$ in area and is assembled using 7 plates of iron (2 A-type with dimensions $2001 \times 1000 \text{ mm}^2$, 2 B-type with dimensions $2001 \times 1000 \text{ mm}^2$, 2 C-type with dimensions $2000 \times 1200 \text{ mm}^2$ and 1 D-type with dimensions $1962 \times 1600 \text{ mm}^2$ as shown in Fig. 2). The C-type plate is slightly narrower than the A-type one, although all of them have the same long edge of 2 m. A gap of about 3 mm, kept fixed using non-magnetic aluminium spacers, is introduced between the iron plates in a layer in order to give access to the (2 mm thick) Hall probe to measure the magnetic field. This provision for measuring the magnetic field measurement is available in only three layers, the 1st (bottom), 6th (middle) and 11th (top) layers. The gap is adjusted to be only 2 mm in the remaining layers¹. While the magnetic field measurement can only be made in the gap between plates, this is expected to be close to the value of the field in the adjacent iron plates. Gaps 0, 2, 3, and 5 (see Fig. 2) are where measurements of the magnetic field have been made. Gaps 1 and 4 are not easy to access.

A current of 500 A is passed through two set of hollow copper coils, located in the coil slots (see Fig. 2), each having 18 turns, with area of cross section $30 \times 30 \text{ mm}^2$. Low conductivity (< 10 micro siemens per cm) cooling water is flowed inside the copper coil for cooling purposes.

2.2 Construction of the Hall probe

The probes can only be inserted in the air gaps of about 3 mm width. From the literature survey, CYSJ106C GaAs Hall Effect Element sensor [6] was found to be suitable for the requirement of Hall probe PCB. The specifications of the sensor are mentioned in Table 1. The probe is constructed

¹These gaps can change when the magnetic field is turned on due to the attractive forces between the magnetized plates.

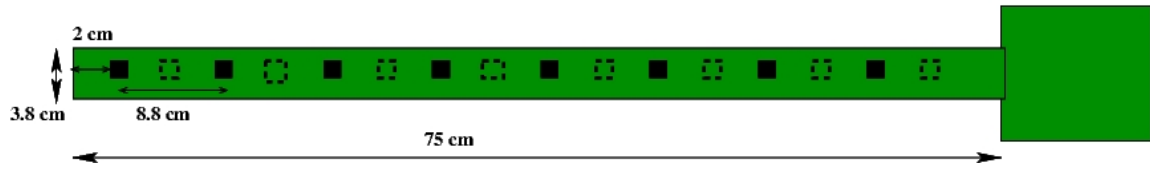


Figure 3. Schematic of the Hall probe, showing the placing of the sensors and the relevant dimensions.

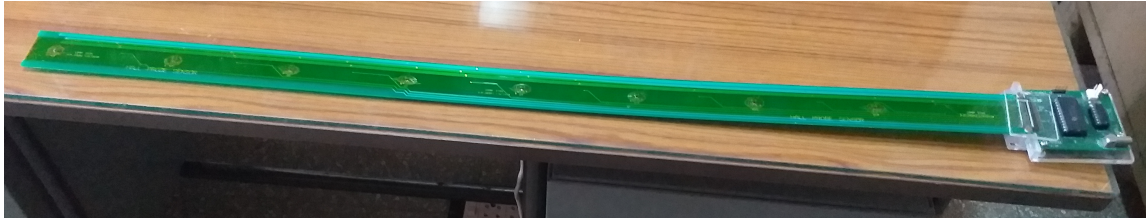


Figure 4. Hall probe PCB with Hall sensors mounted on it.

by mounting 16 Hall sensors labelled 0 to 15, of size $1.5 \text{ mm} \times 1.5 \text{ mm} \times 0.8 \text{ mm}$ (thickness) on a PCB of length 75 cm about 4.4 cm apart, and on alternate sides of it, as shown in Fig. 3; an actual picture is shown in Fig. 4. The thickness of the PCB is 1.2 mm and after mounting the Hall sensors the thickness of PCB becomes 2.3 mm. The sensors are mounted alternatively on the PCB along its length. Therefore when the PCB is placed in a uniform uni-directional field, according to the direction of B -field that a particular sensor faces, half the sensors will show positive value of Hall voltage and other half (mounted on the other side of PCB) will show negative value of Hall voltage. Each sensor is given a number according to their position from the front end electronics. The sensor at the far end from the front end electronics is numbered 0 and the sensor at the near end to the front end electronics is numbered 15.

2.3 Experimental setup

The schematic circuit is shown in Fig. 5. Dual DC power supply of $\pm 5 \text{ V}$ has been used to bias the Hall sensors. All 16 analog Hall voltages are available to read at a time, which are interfaced to the small Analog front end board. The analog front end board consists of a multiplexer, amplifier and buffer. For the sake of simplicity, 16:1 multiplexer has been introduced to the 16 analog readout channels one by one. The IC CD4067-16 analog multiplexer with 4 digital select lines has been used. This IC features low leakage current, lower power consumption and low cross talk between the channels. The output of the multiplexer is connected to a non-inverting amplifier with a gain of 1.045 followed by unity gain amplifier for impedance matching to avoid loading of the output stage. The dual operational amplifier IC LM747N is used to configure the amplifier and buffer. This chip has low power consumption and short-circuit protection. The output is available on a Lemo connector, which can be read out using a digital multimeter or can be given to an ADC with higher resolution. An Arduino Nano board is used to select the Hall sensor channel during manual readout using a digital multimeter.

Parameter	Test Condition	Value
Measurement Range		0–3 T
Max. input power		150 mW
Max input current/voltage		13 mA/10 V
Operating temperature range		–40 ~ 125° C
Hall output voltage	$B = 100\text{mT}$, $I_c = 8\text{mA}$, $V_c = 6\text{V}$	110~150 mV
Offset voltage	$V_c = 6\text{V}$, $B = 0\text{mT}$	$\pm 11\text{ mV}$
Input resistance	$B = 0\text{mT}$, $I_c = 0.1\text{mA}$	650~850 Ω
Output resistance	$B = 0\text{mT}$, $I_c = 0.1\text{mA}$	650~850 Ω
Temperature coefficient of Hall output voltage	$I_c = 5\text{mA}$, $B = 100\text{mT}$	-0.06%/°C
Temperature coefficient of Hall input and output resistance	$I_c = 0.1\text{mA}$, $B = 0\text{mT}$	0.3%/°C
Linearity	$I_c = 5\text{mA}$, $B = 0.1/0.5\text{T}$	2%

Table 1. General characteristics and electrical specifications of the CYSJ106C GaAs Hall sensor [6].

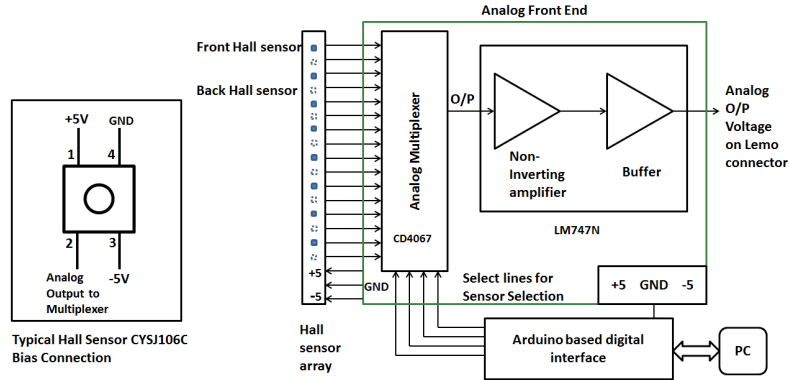


Figure 5. Schematic showing the set up for the Hall probe with the mounted sensors on the left side, the analog front end at the top, and the Arduino digital interface that connects to the PC shown at the bottom.

3 Calibration of the Hall sensors

There are two components to the calibration: one is to determine the offset voltage (the reading of the Hall sensor in the absence of any magnetic field), and the other is to calibrate the Hall voltage to (a known) magnetic field.

3.1 Measurement of the Offset Voltage

The offset voltage arises from the intrinsic properties of the sensor (see Table 1) as well as from the associated electronics. The offset voltage for each sensor is measured in two different ways. In the first approach, the offset of each Hall sensor is measured² keeping the Hall sensor PCB away from the mini-ICAL so that only small stray magnetic fields are present (such as Earth’s magnetic field). These offset measurements were repeated at different times and places. It is observed from Fig. 6

²Since sensors 0 and 15 were defective, results are shown for sensors 1 to 14.

where two typical measurements are shown that there is a small variation in the measured values of the offset.

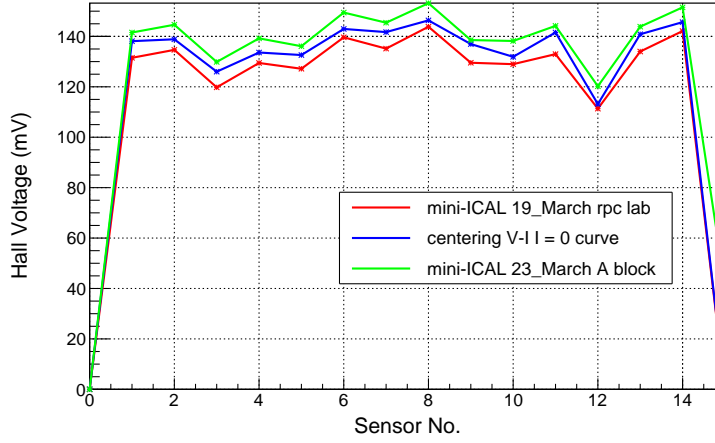


Figure 6. Offset voltage V_0 for each the Hall sensors measured away from mini-ICAL at different places and times (in red and green) in comparison with the offset obtained by centering the $V-I$ curve (in blue); see text for details.

The other way of finding the offset that is implemented here is by centering the $V-I$ curve. The Hall probe was inserted into Gap-2 to the maximum extent, so that Sensor 1 (15) was farthest from (closest to) the edge. The voltage was measured for different values of current over an entire hysteresis loop. It is seen from Fig. 7 that the curve is shifted upward so that an offset V_0 has to be subtracted in order to center the $V-I$ loop; see Fig. 8. This offset was measured for each Hall sensor and is shown in Fig. 6 along with the other measurements of the offset voltage. It is seen that the offset measured in the two different ways follow the same pattern and are consistent with one another. The variation between the measurements of the offset voltage is estimated to be $\Delta V_0 = \pm 5$ mV, and is later used to estimate the errors in the analysis.

Since the Hall sensors are alternatively mounted on opposite sides of the PCB, one set of sensors (even/odd) sees a positive B-field and other set of sensors (odd/even) sees a negative B-field. It was observed that an extra offset $V_\epsilon = 8$ mV has to be added to all the sensors to get agreement between the odd and even set of sensors. This extra offset will be seen to amount to a field of about 0.05 kGauss.

After subtracting the offset voltage, the Hall voltage measured by each sensor is to be converted to a magnetic field measurement. This requires calibration of the sensors by applying a known magnetic field.

3.2 Calibration using gap dipole electro-magnet

An electromagnet calibrator unit that can generate magnetic fields upto 1.5 T (15 kGauss) by varying the current in the coil, is used. The calibration set-up shown in Fig. 9 consists of a set of two copper coils 14 mm in diameter which are mounted on a base. The base can be moved forward and backward on a 1 m length platform using a stepper motor. There are two stoppers named as station 'A' (fixed) and 'B' (moveable) at each end of the platform; see Fig. 10. Clamps are mounted

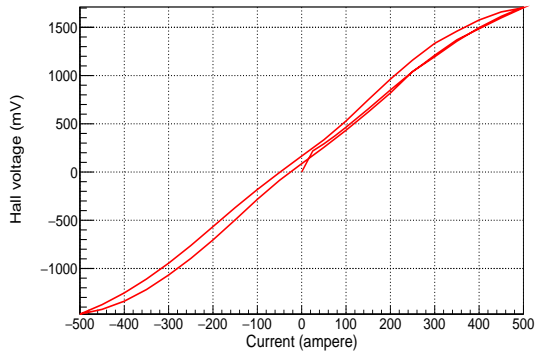


Figure 7. V-I curve for sensor 3 without offset correction.

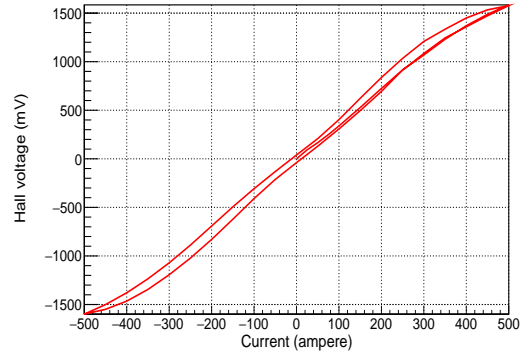


Figure 8. V-I curve for sensor 3 after offset correction.



Figure 9. Calibration Instrument set-up.

on these two stoppers to hold the Hall probe PCB in such a way that a given Hall sensor will be positioned at the center of the poles of the coil which are 2.5 mm apart. This will ensure the sensor sees a uniform and perpendicular field generated by the coils.

The B-field was varied by using different values of current supplied to the coils by a DC regulated power supply (model SVL 030010 D manufactured by the Sairush Electronic Systems). Power supply is used in CC mode to get constant output current from 1 to 4 A in steps of 0.5 A and from 4 to 8 A in steps of 1 A. The B-field generated between the coils is measured using standard gauss meter at different values of the current supplied to the coils. The corresponding Hall voltage of the Hall probe sensor is recorded. This procedure was repeated for each sensor for both ramp-up and ramp-down values of the current. The voltage obtained is plotted against the known magnetic field. A linear relationship was found, as can be seen from the Figs. 11 and 12 plotted for sensor 2 and 7 respectively and the slope m is determined. This was repeated for each sensor. It was found that the typical error on the fit was $\Delta m = \pm 3$ mV/kGauss.

The slopes and intercepts (latter not used in the analysis) for all the Hall sensors are listed in Table 2 for both positive and negative Hall voltages (differing directions of magnetic field). The slope m can then be used to calculate the magnetic field from the measured voltage V as, $B = (V - V_0 + V_\epsilon)/m$.

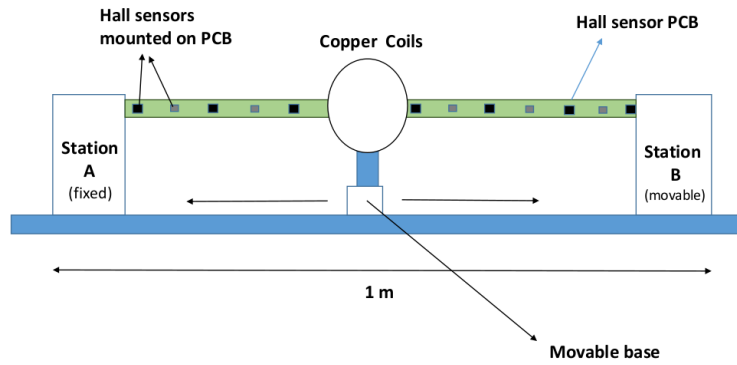


Figure 10. Block diagram of Calibration Instrument set-up.

Sensor no.	Side I		Side II	
	Slope (mV/kGauss)	Intercept (mV)	Slope (mV/kGauss)	Intercept (mV)
1	-150.2	194.7	151.1	-38.19
2	148.2	-35.92	-150.3	207.4
3	-151.9	190.8	151.4	-46.74
4	147.5	-35.38	-150.9	203.1
5	-147.2	188.8	151.2	-52.18
6	148.1	-33.38	-150.6	214.0
7	-149.8	217.1	150.9	-43.7
8	148.7	-26.35	-151.1	227.9
9	-149.1	199.7	151.1	-55.73
10	147.7	-19.88	-150.5	209.2
11	-149.3	222.3	149.7	-40.59
12	149.2	-49.86	-147.6	175.8
13	-151.4	215.5	148.5	-31.91
14	150.3	-27.16	-149.2	212.0

Table 2. Calibration of Hall voltage to magnetic field: the slope and intercept corresponding to each sensor for both positive and negative field values. Side I corresponds to odd sensors facing a negative field while Side II corresponds to odd sensors facing a positive field. The even sensors always see the opposite field.

4 Error Estimation

Before we go on to the actual measurement of the magnetic field in mini-ICAL we make a note of the errors involved. The sources of error we have considered are in the measurement of the offset voltage, ΔV_0 and in the calibration fits to the slope, Δm . Hence the magnetic field B corresponding

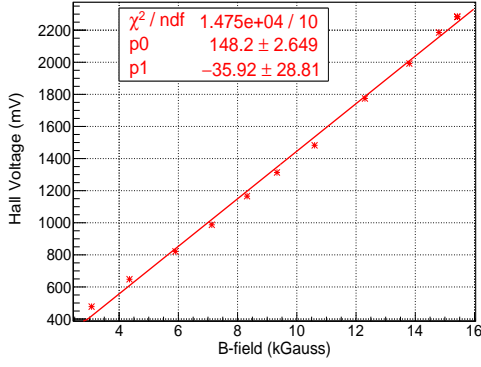


Figure 11. Calibration plot of sensor 2 for positive output voltage.

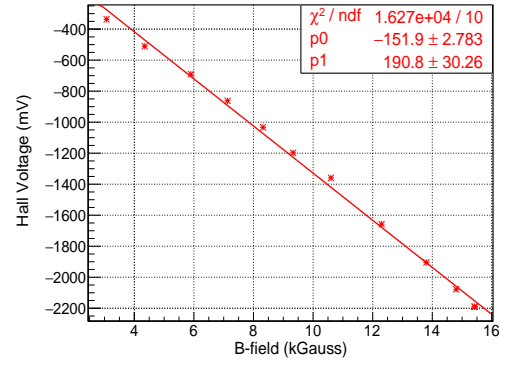


Figure 12. Calibration plot of sensor 3 for negative output voltage.

to a measured voltage of V (and its error δB) is given by

$$B = \frac{V - V_0 + V_\epsilon}{m},$$

$$\delta B = \frac{B}{m} \sqrt{\frac{\Delta V_0^2}{B^2} + \Delta m^2}. \quad (4.1)$$

It can be seen that the error in the measurement of the slope dominates at large values of field while the error in the measurement of the offset voltage dominates at small field values.

5 Measurement of the magnetic field in mini-ICAL

Having completed the calibration of the Hall sensors, we then used them to measure the magnetic field in mini-ICAL. The B-field was measured in the gaps numbered 0, 2, 3 and 5 (see Fig. 2 for reference) in the top layer of mini-ICAL by inserting the Hall probe PCB into these gaps; recall that sensor 1 is closest to the copper coil while sensor 15 is closest to the outside edge of the detector.

The mini-ICAL magnet is ramped up to 500 A using a DC power supply. The Hall voltage measured from each sensor is determined, from which the corresponding magnetic field is calculated as per Fig. 6 and Table 2. This is shown in Fig. 13. Sensor 1 is closer to the copper coil while sensor 14 is closer to the edge and hence the later measures a consistently smaller field in all gaps.

As can be seen from the geometry in Fig. 2, the gaps 0, 2, 3 and 5 are symmetric and ideally should have the same magnetic field (in the x direction, upto a sign). However, in the actual assembly of mini-ICAL plates, these gaps vary in width, with the range shown in Table 3. Therefore the magnetic field is different for these four gaps; the variation in the B-field for sensor 9 is shown as a function of the mean gap width in Fig. 14; as expected, the field value decreases as the gap width increases. Estimating the true value of the magnetic field in the iron plates from the field values in the gap therefore requires detailed simulation, although it is expected to be close to the field value in the gap. This work is on-going and is beyond the scope of the present analysis.

Gap no.	Gap width (mm)	Avg width (mm)
0	3.13-3.23	3.18
2	2.36-3.10	2.73
3	3.15-3.29	3.22
5	2.57-2.86	2.715

Table 3. Measured widths of gaps for Gaps 0, 2, 3, and 5 showing both the range of values and their average.

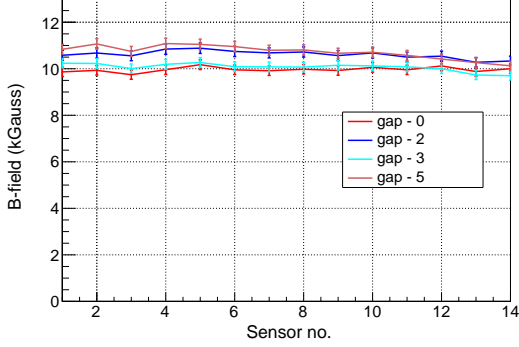


Figure 13. B -field measured in Gaps 0, 2, 3 and 5 by sensors 1–14. Note that sensor 14 typically measures a smaller field due to its location near the outer edge of the detector.

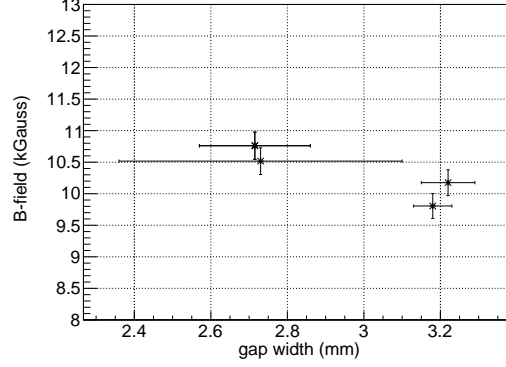


Figure 14. The figure shows the variation of the B -field as a function of the gap width for sensor 9. The field decreases perceptibly as the width increases.

6 Fringe-field just outside mini-ICAL

The fringe field (field outside the iron) is important because it is an indicator of the amount of field leaking out of the detector. The fringe field was measured by inserting the Hall probe into Gap 2 and sliding the probe out by 1 cm at a time upto a distance of $L = 70$ cm. Each sensor measures the magnetic field in its vicinity. Since sensor 14 is closest to the edge, the magnetic field value it measures drops the fastest as it exits the detector into the air, while the magnetic field barely begins to drop for $L = 70$ cm for sensor 1. Hence for convenience, the probe geometry (given in Fig. 3) was used to rescale the sensor position to reflect the distance x from the edge of the detector. Negative values of x indicate that the sensor is still inside the detector dimensions while $x > 0$ indicates the sensor is making measurements in the air outside the detector.

Fig. 15 shows the magnetic field measured by the 14 sensors as a function of the distance x from the detector edge. The field is fairly uniform inside, dropping slightly towards the edge and then dropping rapidly in the air outside the detector. The relatively small fringe field in the air is also shown in close-up view in Fig. 15 on a log scale so that the differences between the field measured by different sensors can be seen. The measurements from different sensors are consistent to within 0.01 kGauss. The errors have been computed as per Eq. 4.1. It can be seen that the fringe field is about $B \sim 0.10 \pm 0.03$ kGauss at $x = 10$ cm and $B \sim 0.04 \pm 0.03$ kGauss at $x = 50$ cm, which is at the limit of sensitivity of the sensor.

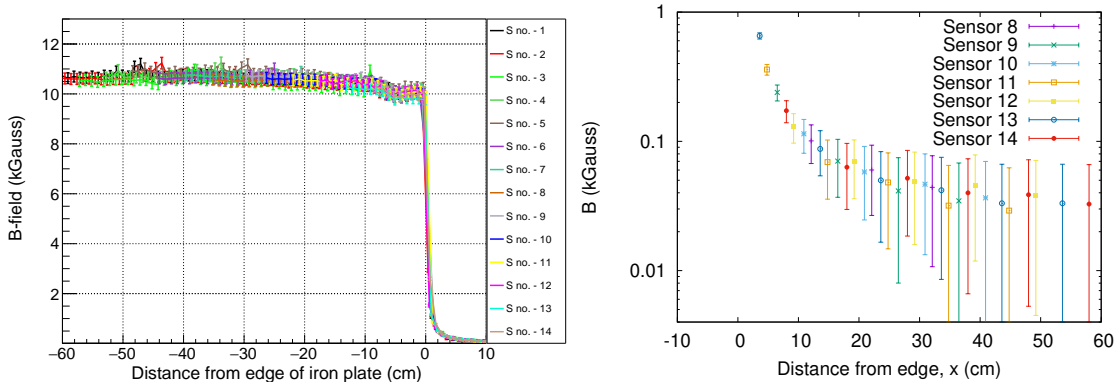


Figure 15. Magnetic field in Gap 2 as a function of the distance x from the edge of the iron plate. Negative values of x indicate the measurement is made inside mini-ICAL while positive values indicate a measurement in the air outside the detector. The figure on the right (y-axis is in log scale) shows a close-up of the smaller fringe fields just outside the detector every 10th point and only a few typical sensors have been plotted for clarity.

7 Discussion and future plans

With a simple, cost-effective design and locally fabricated probes, a measurement of the magnetic field was made in different locations in the mini-ICAL detector. This was the first such detailed measurement of the magnetic field which will play a crucial role achieving the physics goals of the main ICAL detector, including the determination of the neutrino mass ordering/mass hierarchy.

The magnetic field in each layer of mini-ICAL varies in both magnitude and direction across the layer. Since there is provision for measuring the magnetic field in three layers of mini-ICAL (bottom, middle and top) and each layer has 8 air gaps (including two which can accommodate 2 Hall sensor PCBs side by side) to insert Hall probe PCBs, the future plan is to make 30 such PCBs to make a precision measurement of the magnetic field in different locations in mini-ICAL. An automated system will be developed for the data acquisition from the Hall probe PCBs so that magnetic field from all the gaps can be measured and recorded simultaneously.

Additionally, the magnetic field has currently been measured in the linear, not saturation, region of the B - H curve since the maximum current that can be supplied to the coils is 500 A; this can generate a field of ~ 10.5 kG. In the future we plan to measure the magnetic field at saturation values of about 15 kG using a current of ~ 900 A by installing a power supply which can provide currents of upto 1000 A. We will also compare the measured and simulated magnetic fields that will be an important input to determine a detailed magnetic field map for both the mini-ICAL and main ICAL detectors.

A Calibration of Hall probe at 90° dipole magnet at ECR ion source facility.

The Electron Cyclotron Resonance (ECR) lab in TIFR has a 90° bending dipole electromagnet that is used to select ions having the same mass/charge (M/Q) ratio. The maximum field that can be produced in it is 3 kG. The system is controlled using LabVIEW software. The photograph of the dipole magnet is shown in Fig-16.

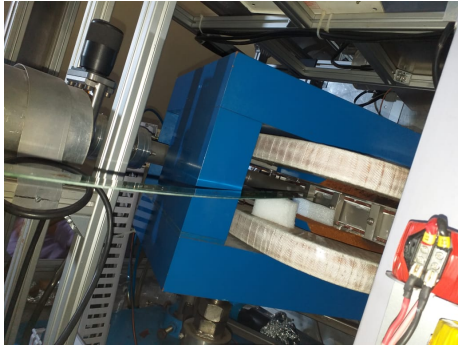


Figure 16. ECR Ion source magnet.

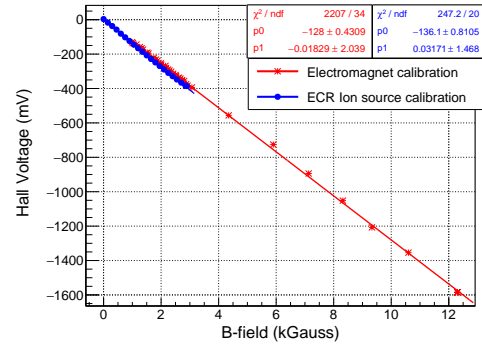


Figure 17. Comparison of the calibration done using electromagnet and ECR Ion source magnet.

The Hall probe PCB is placed in the middle of the two coils and oriented such that the Hall probe is perpendicular to the magnetic field. The field is increased in steps of 150 Gauss and corresponding Hall voltage in the Hall sensor is noted (see Fig. 17). The Hall voltage vs magnetic field data is plotted and fitted to a straight line for a field upto 3 kG. The measurement is shown in Fig. 17 along with the calibration using the gap dipole electromagnet discussed in Section 3. A reasonable consistency is seen at the lower values of the field, $B \leq 3$ kG, *i.e.*, in the overlapping regions of measurement.

References

- [1] Shakeel Ahmed et al., ICAL collab., INO White Paper, *Pramana* **88** (2017) 5, 79; arXiv: 1505.07380 [physics.ins-det].
- [2] D. Indumathi and M. V. N. Murthy, "A question of hierarchy: matter effects with atmospheric neutrinos and anti-neutrinos", 10.1103, *Phys. Rev.* **D 71** 013001, arXiv: hep-ph/0407336 [hep-ph].
- [3] Shiba P Behera et al., *IEEE Transactions on Magnetics* **51**, 7300409 (2014).
- [4] B. Satyanarayana et al., "Hall Sensor Array based Magnetic Field Measurement System", *International Journal of Instrumentation Electrical and Electronics Engineering (IJIEEE)* (2019).
- [5] Honey et al., "Magnetic field simulations and measurements on mini-ICAL", XXIV DAE-BRNS HIGH ENERGY PHYSICS SYMPOSIUM, 2020.
- [6] Data sheet CYSJ106C, ChenYang Technologies GmbH and Co. KG, Version 2 Released in May 2016.